

## Observation of Nonclassical Radial Current Diffusion in a Fully Bootstrap Current Driven Tokamak

Y. S. Hwang, C. B. Forest,\* and M. Ono

Princeton University, P.O. Box 451, Princeton, New Jersey 08543

(Received 18 December 1995)

Reconstruction and modeling of the plasma current profiles in a fully pressure driven tokamak have been performed in the Current Drive Experiment-Upgrade. The reconstructed experimental current profile has a significant deviation from that of the calculated neoclassical currents. Satisfactory agreement between the measured and calculated model profiles was obtained by including a helicity conserving current diffusion term in the modeling which created the required self-generated “seed” current. [S0031-9007(96)01380-4]

PACS numbers: 52.55.Fa, 52.25.Fi

For future long-pulse and/or steady-state tokamaks, internally generated bootstrap current is expected to play a major role since it could reduce the requirements for non-inductive current drive. Theoretical estimates show that a large fraction of plasma current is expected to flow as bootstrap current in high beta-poloidal ( $\beta_{\text{pol}}$ ) reactor-grade plasmas [1]. Recent experimental observations in high- $\beta_{\text{pol}}$  tokamak plasmas heated by neutral beam injection (NBI) [2,3] electron cyclotron heating (ECH) [4], and ion cyclotron range of frequency (ICRF) [5] support this prediction. It is generally believed that the bootstrap current requires a “seed” current near the plasma magnetic axis since no neoclassical current is expected to be generated there except in limited conditions [6]. However, the possibility of sustaining tokamak plasmas solely by bootstrap current has been suggested previously [7,8]. Several non-classical mechanisms of transporting the bootstrap current to the magnetic axis have been proposed, thereby permitting bootstrap current to be self-sustained. A fully self-sustaining tokamak, if possible, is indeed very attractive as a simple economic reactor option.

It has been reported that the flux surface closure was achieved in the Current Drive Experiment-Upgrade (CDX-U) experiment entirely by pressure-driven currents ( $I_p \leq 1$  kA) with a toroidal mirror configuration shown in the left of Fig. 1 [9]. The toroidal magnetic field strength was varied between 600 and 900 G, which was required to have ECH resonance for 2.45 GHz in the plasma. Typical plasma current of about 1 kA was supported by constant vertical field at the toroidal field of 600 G, giving  $q_a \approx 30$  with  $R = 38$  cm and  $a = 22$  cm. With the ECH power of 8 kW, electron density and temperature reached  $10^{11}$  cm $^{-3}$  and 30 eV, respectively, which provided high beta poloidal ( $\beta_{\text{pol}} \approx 1.6$ , i.e.,  $\epsilon\beta_{\text{pol}} \approx 1$ ) and low collisionality plasmas. Time traces of discharges with constant poloidal and toroidal fields are given in Fig. 2. Plasma current reaches steady state at  $t \approx 20$  msec. Measured wall eddy currents, shown in Fig. 2(b), evolve with the wall resistive skin time of about 10 msec. The discharge after reaching a true steady state is maintained for an excess of 10 msec, which is much longer than the

plasma energy confinement time, the plasma particle confinement time, and resistive skin time. With discharge optimization and vertical field programming, up to 2.4 kA of pressure driven current with  $q_a$  of  $\approx 12$  has been obtained from zero current when nonphased 8 kW of ECH power was applied.

An important question we attempt to answer in this Letter is how such a plasma can be generated and sustained self-consistently, and how well the existing neoclassical or other theoretical models explain the experimental observation. For this investigation, we have developed and applied a two-dimensional profile reconstruction technique from detailed magnetic and kinetic diagnostic systems and compared with the neoclassical model calculations. A crucial discrepancy between the experimental observation and the neoclassical model lies in the current profiles, where the former shows smooth and nonhollow and the latter shows hollow characteristics. In this Letter, we report that satisfactory agreement between the measured and calculated profiles is obtained when the helicity conserving current diffusion term of Boozer [10] is included in the modeling. This result supports the existence of a nonclassical helicity

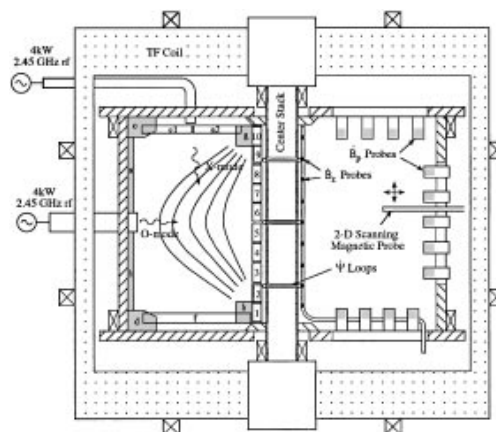


FIG. 1. A schematic of CDX-U experimental setup. The left side shows isolated limiters around the poloidal direction and ECH setup, and the right side is magnetic diagnostics including a two-dimensional scanning probe.

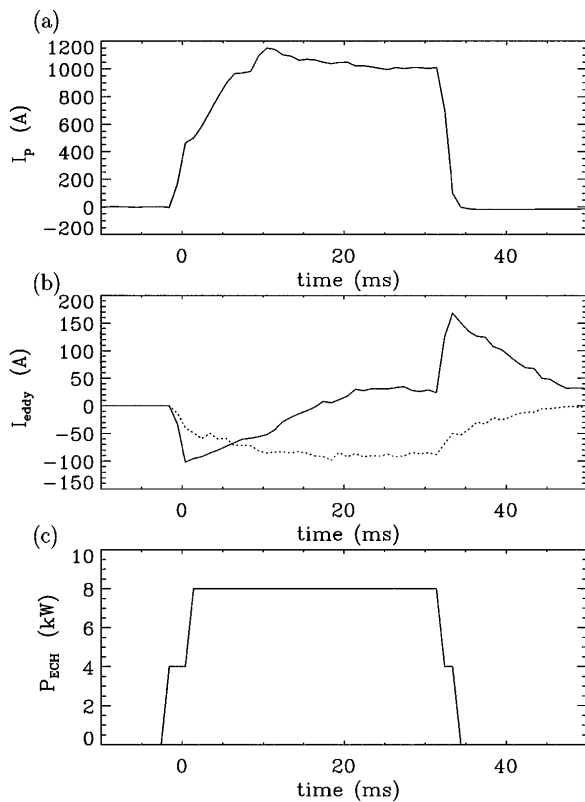


FIG. 2. Temporal evolution of typical discharges with constant toroidal and poloidal magnetic fields. (a) Plasma current evolves for the duration of the ECH heating pulse and reaches steady state for more than 20 msec. (b) Vacuum vessel eddy currents measured by Rogowski loops at two different poloidal sections (one most resistive and the other most conductive section) shows wall resistive skin time of less than 10 msec, showing discharge reached actual steady state of more than 10 msec. (c) Applied ECH power during the discharge.

conserving current transport mechanism which generates seed current near the plasma axis to sustain a fully pressure driven tokamak discharge [7,8].

To model the neoclassical currents, a two-dimensional magnetic field structure and pressure profiles are required. The current density distributions are reconstructed from internal and external magnetic measurements from the magnetic diagnostic array as shown on the right of Fig. 1 by averaging multiple shots with small shot-to-shot variations of less than a few percent [11]. Three-dimensional magnetic pickup coils, located at 13 different poloidal positions, measure the vector magnetic field. Three flux loops are wound around the central toroidal field column (center stack) to provide poloidal magnetic flux measurements at the inside boundary. Nine one-dimensional pickup coils are located near the center stack to measure the vertical magnetic field. A two-dimensionally scannable magnetic probe system [12] maps poloidal magnetic fields radially from  $R = 36$  to 60 cm and vertically from  $Z = -13$  to 16 cm. The external magnetic measurements describe above together with the limited internal probe measurements with the perturbation of less

than 5% in total plasma currents can reconstruct the current density distributions with total experimental errors of less than 20% by taking advantage of the low-aspect-ratio nature of the plasma, utilizing a least squares error technique and a finite element method [11,13,14]. Reconstructed current density and magnetic flux contours are shown in Fig. 3. Formation of a low-aspect-ratio tokamak configuration can indeed be seen. Also, the reconstructed current density profiles at midplane are compared with current densities calculated directly from radial and vertical magnetic fields measured by two-dimensionally scanning internal probes, showing good agreement at the plasma edge as shown in Fig. 4(c). Electron density profiles are measured two dimensionally by a 140 GHz interferometer system [15]. This microwave interferometer scans horizontally from 26 to 55 cm and vertically from  $-22$  to  $+22$  cm, which is limited by the size of rectangular ports on the vacuum vessel. An additional channel is installed inside the vacuum vessel at  $R = 17$  cm. Imposing the known magnetic structure as a grid, a tomographic inversion of electron density was performed by using a least squares error technique [14]. The reconstructed density profile agreed well with the local Langmuir probe measurements as shown in Fig. 4(a). The radial profile of electron temperature shown in Fig. 4(b) was obtained at midplane by using a small cylindrical Langmuir probe made of 0.4 mm tungsten wire. These density and temperature profiles with the reconstructed magnetic structure are used to model neoclassical currents.

We first describe the physics of neoclassical current generation in CDX-U. A toroidal mirror configuration shown in the left of Fig. 1 has been utilized to provide initial confinement for a hot, ECH-produced, trapped electron population [9]. For the open field line configuration, a precessional current comprises most of the toroidal current. Given the pressure profile and the poloidal field strength, the precessional current density can be estimated as  $J_{\text{prec}} \approx P_e/RB_{\text{pol}}$ , where  $P_e$ ,  $R$ , and  $B_{\text{pol}}$  are electron pressure, major radius, and poloidal field, respectively [16]. It is important to note the role of the Pfirsch-Schluter

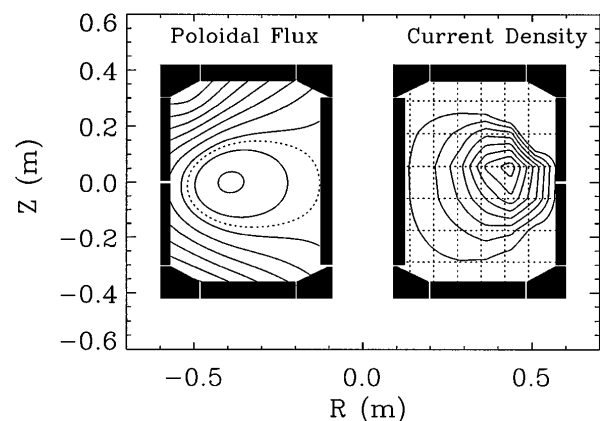


FIG. 3. Magnetic flux and current density contours reconstructed from the magnetic diagnostic data.

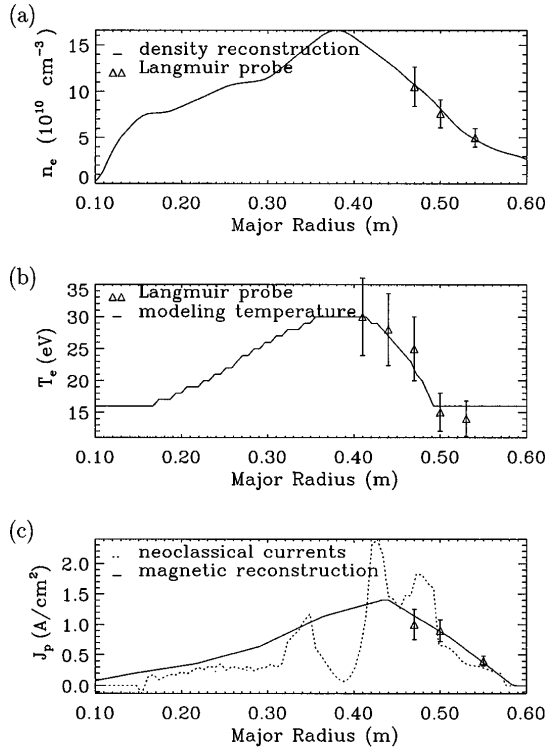


FIG. 4. Measured and reconstructed midplane profiles. (a) Density profiles reconstructed from the two-dimensional interferometer system with local Langmuir probe data shown for comparison. (b) Electron temperature profile reconstructed from the Langmuir probe data. (c) Comparison of the reconstructed and calculated neoclassical current density profiles. Local current densities measured by scanning magnetic probes show good agreements with the reconstructed profiles.

(PS) current which is generated by the pressure gradients. This current consists of a codirected current in the outer region and a counter directed current in the inner region, producing a negative vertical field in the central region. Although the PS current itself does not carry a significant net toroidal current, it reduces the vertical field substantially in the central high pressure region, which can then enhance the precession current as much as a factor of 2. With inclusion of both precessional and Pfirsh-Schluter currents, the estimated neoclassical current level agrees satisfactorily with the measured total plasma current in this low-current, open-field-line configuration.

After the closed flux surface formation, previously trapped electrons start to be detrapped and become passing particles since the mirror ratio generally decreases inside the flux tube. With increasing numbers of passing particles, the bootstrap current becomes a major contributor to the plasma current, while precession current contribution tends to decrease. Indeed, after the closing of the flux surface ( $I_p \approx 600 \text{ A}$ ), the current can spontaneously increase further to  $I_p \approx 1 \text{ kA}$  due to bootstrap current. The bootstrap current  $J_{bs}$  at an arbitrary aspect ratio is given in Ref. [17]. Here ions are considered to be cold. In addition, when there is an

in-out asymmetry of electron density in the same flux surface, electrostatic trapping can take place and enhance neoclassical transport [18]. After taking various effects into account, we still find the measured total plasma current in this closed-field-line configuration to be larger by  $\approx 20\%$  than the calculated total neoclassical currents. The collisional effect, though not included in our model due to low collisionality, tends to reduce the bootstrap current and, thus, cannot explain this discrepancy. However, this systematic deviation is still within the experimental uncertainty in estimating the effective  $T_e$  in the ECH heated discharges using a Langmuir probe since ECH heated plasmas can develop nonthermal energetic electron population [19]. These energetic electrons can contribute significant pressure driven currents and can explain the discrepancy in the total plasma current.

The most significant discrepancy between measurements and neoclassical model, however, is in the qualitative nature of the current profiles. The expected current density profiles calculated from neoclassical theory show a hollow characteristic, whereas the reconstructed current density profiles are nonhollow as shown in Fig. 4(c). The midplane vertical magnetic field measured by the internal probe also supports this deviation. To resolve this discrepancy, nonclassical current transport is considered. An anomalous viscosity term is introduced into Ohm's law with the helicity conserving form [10] as following:

$$\mathbf{E} + \mathbf{u} \times \mathbf{B} = \eta(\mathbf{j} - \mathbf{j}_{nc}) - \frac{\mathbf{B}}{B^2} \nabla \cdot \left( \lambda \nabla \frac{j}{B} \right), \quad (1)$$

with  $\eta$  the classical Spitzer resistivity,  $\mathbf{j}_{nc}$  the neoclassical current density, and  $\mathbf{j} = (j/B)\mathbf{B}$  the current density. The hollow current profile, for example, is generally believed to be unstable against the double tearing mode which can induce the nonclassical current diffusion [20]. This nonclassical diffusion term can redistribute current to the magnetic axis, so that nonhollow current density profiles can be obtained. Here  $\lambda$  represents a current viscosity which determines the current density profile for a given pressure profile. With this nonclassical current penetration, self-consistent modeling is attempted. Parallel force balance from Ohm's law with Faraday's law and Ampere's law gives a current transport equation,

$$\frac{\partial j}{\partial t} = \frac{\eta}{\mu_0} \nabla^2 (j - j_{nc}) - \frac{1}{\mu_0} \nabla^2 \left[ \frac{1}{B_T} \nabla \cdot \left( \lambda \nabla \frac{j}{B_T} \right) \right], \quad (2)$$

assuming  $B \approx B_T$ . Using the calculated neoclassical current  $j_{nc}$  as an initial value for each time step, the helicity conserving current transport is estimated with the time step of  $10^{-3} \tau_s$  in the experimental toroidal geometry. Here a plasma skin time is  $\tau_s = \mu_0 a^2 / \eta$ . The neoclassical current is recalculated for the new magnetic structure obtained from the updated current density  $j$ , so self-consistent current density profiles are obtained for different  $\lambda$  values as shown in Fig. 5(a). Here the total plasma current is maintained constant as constraints by the experimental value.

The vertical fields at the midplane from these current density profiles are compared with the fields measured by the internal magnetic probe. Figure 5(b) shows the comparison for different  $\lambda$  values. With a small value of  $\lambda$ , nonclassical current transport is not sufficient to balance the bootstrap effect which tends to push the poloidal magnetic field out of the regions of high plasma pressure as shown in Fig. 5(b) and makes a current density profile become more hollow as time goes on. In this case, plasma current should not be maintained longer than the resistive time scale, which is inconsistent with our experimental observations. With the sufficient nonclassical current transport of a larger viscosity, nonhollow profiles are maintained. However, too large viscosity tends to move current density toward high field side, which is inconsistent with magnetic measurements as shown in Fig. 5(b). The nonhollow profile with anomalous viscosity of about 20% of  $R_0^2 B_0^2 \eta$  shows a good agreement with the experimental measurements. We should note that this observation is reminiscent of the previous helicity injection experiment where the nonhollow profile was observed even with the edge current drive [21]. Other possible mechanisms for generating the central seed currents are externally provided electric fields and finite particle banana effects [8]. The magnitude of vacuum vessel eddy currents is too small to

generate sufficient central current density, and discharges are maintained much longer than the measured eddy current skin time. Also, the width of electron bananas is relatively large (about 1 cm), but much smaller than plasma minor radius. This excludes the possibility of finite banana effects.

In conclusion, a fully bootstrap current driven tokamak plasma was examined using a self-consistent model utilizing reconstructed 2D pressure and magnetic flux profiles. By introducing a helicity conserving nonclassical current transport model, the observed self-maintenance of neoclassical bootstrap currents was explained. This finding supports earlier theoretical predictions of a tokamak discharge maintained entirely by internally generated currents [7,8].

The authors would like to acknowledge the CDX-U group. Also, Dr. S.C. Jardin and Dr. C.S. Chang have provided helpful suggestions. This work was supported by the U.S. Department of Energy under Contract No. DE-AC02-76-CHO-3073.

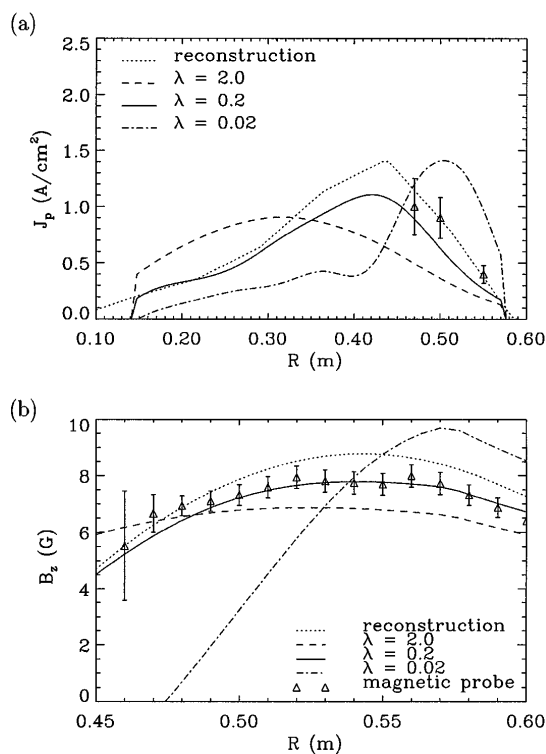


FIG. 5. Nonclassical current diffusion. (a) Current density profiles at the midplane for different anomalous viscosity factors. The anomalous viscosity is in units of  $R_0^2 B_0^2 \eta$ . (b) Vertical magnetic fields at the midplane for different anomalous viscosity factors are compared to those measured by the internal probe.

- \*Current address: General Atomics, San Diego, CA 92186.
- [1] R. J. Bickerton, J. W. Connor, and J. B. Taylor, *Nature* (London) **229**, 110 (1971).
  - [2] M. C. Zarnstorff *et al.*, *Phys. Rev. Lett.* **60**, 1306 (1988).
  - [3] M. Kikuchi, *Nucl. Fusion* **30**, 265 (1990).
  - [4] V. Alikaeiev *et al.*, in *Radio Frequency Power in Plasmas*, edited by Donald B. Batchelor, AIP Conf. Proc. No. 244 (AIP, New York, 1991) p. 11.
  - [5] C. D. Challis *et al.*, Joint European Torus, Technical Report No. JET-P(92)76 1992.
  - [6] C. S. Chang, in *Proceedings of the 14th IAEA Conference, Wurtzburg, Germany, 1992* (IAEA, Vienna, Austria, 1993), Vol. I, 759.
  - [7] R. H. Weening and A. H. Boozer, *Phys. Fluids B* **4**, 159 (1991).
  - [8] Ya. I. Kolesnichenko, D. Anderson, M. Lisak, and H. Wilhelmsson, *Phys. Rev. Lett.* **53**, 1825 (1984).
  - [9] C. B. Forest, Y. S. Hwang, M. Ono, and D. S. Darrow, *Phys. Rev. Lett.* **68**, 3559 (1992).
  - [10] A. H. Boozer, *J. Plasma Phys.* **35**, 133 (1986).
  - [11] Y. S. Hwang, C. B. Forest, D. S. Darrow, G. Greene, and M. Ono, *Rev. Sci. Instrum.* **63**, 4747 (1992).
  - [12] G. J. Greene and M. Ono, *Bull. Am. Phys. Soc.* **34**, 1993 (1989).
  - [13] F. Hofmann and G. Tonetti, *Nucl. Fusion* **28**, 519 (1988).
  - [14] Y. S. Hwang, Ph. D. thesis, Princeton University (1993).
  - [15] C. B. Forest, G. J. Greene, and M. Ono, *Rev. Sci. Instrum.* **61**, 2888 (1990).
  - [16] K. Miyamoto, *Plasma Physics for Nuclear Fusion*, (MIT Press, Cambridge, MA, 1976), pp. 65–70.
  - [17] P. Hirshman, *Phys. Fluids* **31**, 116 (1988).
  - [18] C. S. Chang, *Phys. Fluids* **26**, 2140 (1983).
  - [19] W. Choe, C. S. Chang, and M. Ono, *Phys. Plasmas* **2**, 2044 (1995).
  - [20] T. H. Stix, *Nucl. Fusion* **18**, 353 (1978).
  - [21] M. Ono *et al.*, *Phys. Rev. Lett.* **59**, 2169 (1987).